

Exploring the evolution of spiral galaxies

Eric F. Bell^{1,2,3} and Richard G. Bower^{1,4}

¹ Department of Physics, University of Durham, Science Laboratories, South Road, Durham DH1 3LE, UK

² Steward Observatory, University of Arizona, 933 N. Cherry Ave., Tucson, AZ 85721, USA

³ ebell@as.arizona.edu

⁴ r.g.bower@durham.ac.uk

RE-SUBMITTED TO MNRAS 12 MAY 2000

ABSTRACT

We have constructed a family of simple models for spiral galaxy evolution to allow us to investigate observational trends in star formation history with galaxy parameters. The models are used to generate broad band colours from which ages and metallicities are derived in the same way as the data. We generate a grid of model galaxies and select only those which lie in regions of parameter space covered by the sample. The data are consistent with the proposition that the star formation history of a region within a galaxy depends primarily on the local surface density of the gas but that one or two additional ingredients are required to fully explain the observational data. The observed age gradients appear steeper than those produced by the density dependent star formation law, indicating that the star formation law or infall history must vary with galactocentric radius. Furthermore, the metallicity–magnitude and age–magnitude correlations are not reproduced by a local density dependence alone. These correlations require one or both of the following: (i) a combination of mass dependent infall *and* metal enriched outflow, or (ii) a mass dependent galaxy formation epoch. Distinguishing these possibilities on the basis of current data is extremely difficult.

Key words: galaxies: spiral – galaxies: stellar content – galaxies: evolution – galaxies: general

1 INTRODUCTION

The chemical evolutionary histories of spiral galaxies provide considerable insight into many of the important processes involved in galaxy formation and evolution. For example, we can study star formation laws (SFLs; e.g. Wyse & Silk 1989; Phillipps & Edmunds 1991), the interactions between newly-formed stars and the interstellar medium (e.g. Dekel & Silk 1986; MacLow & Ferrera 1999), the importance and effects of gas flows (e.g. Lacey & Fall 1985; Edmunds 1990; Edmunds & Greenhow 1995) and the infall that must accompany disc formation (e.g. Tinsley & Larson 1978; Lacey & Fall 1983; Steinmetz & Müller 1994). The main challenge is obtaining *unambiguous* insight into particular physical processes. Some of the ambiguity can be circumvented by studying both the ages and the metallicities of galaxies: in this paper we use the ages and metallicities of a sample of face-on spiral galaxies to constrain which processes are the most important in affecting their observational properties.

Despite these difficulties, considerable progress has been made in understanding some important aspects of galaxy formation and evolution. A local density dependence in the SFL is strongly favoured, although other factors may af-

fect the star formation rate (SFR) over galactic scales (e.g. Schmidt 1959; Dopita 1985; Kennicutt 1989; Wyse & Silk 1989; Dopita & Ryder 1994; Prantzos & Aubert 1995; Kennicutt 1998). Infall may be important in determining the metallicity distribution of stars in the solar neighbourhood (e.g. Tinsley 1980; Prantzos & Aubert 1995; Pagel 1998). Other processes are more controversial: e.g. metal-enriched outflows (e.g. MacLow & Ferrera 1999) or radial gas flows (e.g. Edmunds & Greenhow 1995; Lacey & Fall 1985).

However, recent observational advances, coupled with the development of multiple metallicity stellar population synthesis codes has allowed comparison of galaxy evolution models with both the gas metallicities and colours of spiral galaxies (Contardo, Steinmetz & Fritz-von Alvensleben 1998; Jimenez et al. 1998; Boissier & Prantzos 2000; Prantzos & Boissier 2000; Cole et al. 2000). The colours of spiral galaxies depend on both their ages and metallicities, therefore study of their colours offers fresh insight into galaxy formation and evolution, although inevitably degeneracies remain.

In Bell & de Jong (2000; BdJ hereafter), we analysed the optical–near-infrared (near-IR) colours of a sample of

121 low-inclination spiral galaxies in conjunction with up-to-date stellar population synthesis models to explore trends in age and metallicity with galaxy parameters, such as magnitude or surface brightness. In particular, we found that there are significant trends between the age and K band surface brightness of a galaxy, and between the metallicity and both the K band magnitude and surface brightness of a galaxy. In that paper, we argued that these correlations could be the result of a surface density-dependent SFL, coupled with galaxy mass-dependent chemically-enriched gas outflows.

In this paper, we investigate these ideas in more detail. We use a family of simple models to explore the effects of infall, outflows, age differences and SFLs on the colour-based ages and metallicities of spiral galaxies. Our aim is not to construct a self-consistent, realistic model of galaxy formation and evolution. This work is intended to guide future, more detailed explorations of the star formation histories (SFHs) of spiral galaxies: this simple modelling isolates which physical processes affect which observables, to allow more realistic models to concentrate on formulating self-consistent prescriptions for the most important physical phenomena.

The plan of this paper is as follows. In section 2, we outline the data and its main limitations. We describe the chemical evolution model, the basic assumptions and equations and outline how we translate the model output into observables which we can readily compare with the data. In section 3, we describe the properties of the closed box model. In section 4 we explore the effects of infall, outflow and systematic trends in galaxy formation epoch. In section 5, we investigate the effects of changing the SFL on our results. In section 6 we discuss the results further, checking the plausibility of these models with other observational constraints. There, we also compare our models to a comparable, but more detailed model by Boissier & Prantzos. Finally, in section 7, we summarise our results.

2 THE METHOD

2.1 The data

For this paper, we use the sample of 121 low-inclination spiral galaxies from BdJ. The sample is described in more detail in BdJ and in the sample's source papers (Bell et al. 2000; de Jong & van der Kruit 1994; Tully et al. 1996). The sample galaxies were chosen to have radially-resolved surface brightnesses in at least one near-IR and two optical passbands. The sample galaxies have a wide range of surface brightnesses, magnitudes, scale lengths and gas fractions, but are not complete in any statistical sense (at least as a unit).

In BdJ, we used a combination of at least one near-IR and two optical passbands to split (to some degree) the age-metallicity degeneracy. We fit simplified SFHs to the optical–near-IR colours using a maximum likelihood technique to derive crude age (reflecting the amount of recent to past star formation; c.f. a birthrate parameter) and metallicity estimates. These estimates are not accurate in an absolute sense: they are subject to uncertainties from a number of sources including model uncertainties, the effects of small bursts of star formation, the assumption of a single epoch

of galaxy formation 12 Gyr ago and dust, to name a few. However, we argue that the estimates are robust in a relative sense: these uncertainties compromise the absolute ages and metallicities but leave the relative ranking of galaxies by age or metallicity relatively unaffected.

The ages and metallicities of one scale length wide annuli in our sample galaxies were estimated using the above method. We also constructed estimates of the age and metallicity at one disc half-light radius and their gradients per K band scale length using a weighted linear fit to the ages and metallicities as a function of radius. More description of the method, its caveats and limitations can be found in BdJ.

2.2 Basic assumptions and equations

In order to make the investigation of the trends in age and metallicity a tractable problem, we adopt highly simplified *ad hoc* prescriptions describing star formation and galaxy evolution. These simple approximations allow us to investigate which effects play an important role in e.g. imprinting mass dependence in the SFH. We *do not* include gas flows in these models: assuming that the final total baryonic mass distribution is no different from a model without gas flows, the primary difference between models with and without gas flows will be the metallicity gradients (e.g. Lacey & Fall 1985; Edmunds 1990; Edmunds & Greenhow 1995). Therefore, the metallicity gradients are not iron-clad constraints on the models (in any case, the metallicity gradients are relatively unaffected by many of the changes explored in this paper, so the metallicity gradients were not particularly strong model constraints anyway).

For consistency with our age and metallicity estimation procedure, we assume that our model galaxy forms 12 Gyr ago as an exponential disc of gas with surface density $\Sigma_0(r) = \Sigma_0(r=0)e^{-r}$, where Σ_0 is the initial surface density of gas in $M_\odot \text{ pc}^{-2}$, and r is the radius in units of the scale length of the gas (denoted by h). For the infall case (see section 4.1), $\Sigma_0(r) = 0$ initially, and the gas mass is gradually built up over time assuming an exponentially declining infall rate with e -folding time τ_{infall} . For the case in which we allow the galaxy formation epoch to vary as a function of its mass (see section 4.3), we change the galaxy formation epoch from 12 Gyr to between 4 and 12 Gyr, depending on galaxy mass.

The gas forms stars according to a prescribed SFL: in much of this paper we adopt a Schmidt (1959) SFL in terms of the gas surface density Σ_{gas} :

$$\psi = k\Sigma_{\text{gas}}^n, \quad (1)$$

where ψ is the SFR in $M_\odot \text{ pc}^{-2} \text{ Gyr}^{-1}$, k is the efficiency of star formation at a gas surface density of $1 M_\odot \text{ pc}^{-2}$ and n is the exponent specifying how sensitively the SFR depends on gas surface density.

This star formation produces heavy elements; here we adopt the instantaneous recycling approximation (IRA; e.g. Tinsley 1980; Pagel 1998). A fraction R of the mass of newly formed stars is instantaneously returned to the gas. We adopt a Salpeter (1955) initial mass function (IMF) with lower and upper mass limits of $0.1 M_\odot$ and $125 M_\odot$ respectively to describe the chemical and photometric evolution of our stellar populations: for this IMF the returned fraction $R \sim 0.3$. This gas is returned along with a mass

$p\psi(1 - R)$ of heavy elements, where p is the true yield, and is defined as the mass of freshly produced heavy elements per unit mass locked up in long-lived stars. The true yield p is taken to be 0.02 (solar metallicity) hereafter unless explicitly stated otherwise. Note that, for simplicity, we assume a metallicity-independent yield. Note that our use of the IRA should not lead to significant inaccuracies, as the metallicity of spiral galaxies is typically measured via their oxygen content: for oxygen, the IRA is a fairly accurate approximation as it is produced primarily by Type II supernovae (c.f. Pagel 1998; although this assumption breaks down at late stages of galactic evolution near gas exhaustion; Portinari & Chiosi 1999; Prantzos & Boissier 2000).

Once the IRA is adopted, the following three equations specify the evolution of the galaxy completely:

$$\frac{d\Sigma_{\text{gas}}}{dt} = F - E - \psi(1 - R) \quad (2)$$

$$\frac{d\Sigma_{\text{stars}}}{dt} = \psi(1 - R) \quad (3)$$

$$\frac{d(\Sigma_{\text{gas}}Z)}{dt} = p\psi(1 - R) - Z\psi(1 - R) - Z_E E + Z_F F, \quad (4)$$

where Σ_{stars} is the surface density of the stars in $\text{M}_\odot \text{ pc}^{-2}$, F is the gas surface density infall rate (with an initial metallicity Z_F ; we assume $Z_F = 0$ hereafter) in $\text{M}_\odot \text{ pc}^{-2} \text{ Gyr}^{-1}$, E is the surface density of gas ejected in outflows (with metallicity Z_E) in $\text{M}_\odot \text{ pc}^{-2} \text{ Gyr}^{-1}$ and Z is the gas metallicity (Tinsley 1980; Pagel 1998).

2.3 Determining ages and metallicities

We follow the evolution of the galaxy using a numerical scheme with a 20 Myr timestep. We split our model galaxies into 20 radial zones between $r = 0$ and $r = 4$ gas disc scale lengths, to allow study of both global and radial trends in age and metallicity. While some of the cases we study here have analytical solutions, our use of a numerical scheme allows us to use more complex SFLs and e.g. infall or outflow histories.

In order to properly compare the models with the data, we use the colour-based maximum-likelihood technique from BdJ to determine the ages and metallicities of our model galaxies. In order to use this technique, we must have a set of optical and near-IR colours for our model galaxies. Therefore, in each zone at each timestep, we use the *total* mass of newly-formed stars (both short- and long-lived) to compute the contribution of those stars to the total flux at the present day in U , B , V , R , I , J , H and K bands using interpolations between the multi-metallicity GISSLE98 models of Bruzual & Charlot (in preparation).

We then use these local colours as input to the maximum-likelihood age and metallicity estimator developed for and presented in BdJ. In this way, *we obtain model ages and metallicities determined in exactly the same way as the observations we compare with*. This can be quite important: especially so for older stellar populations. Mass-weighted average ages of older stellar populations can differ considerably from the luminosity-weighted ages derived using the colour-based technique because of only relatively modest amounts of recent star formation.

Using these local age and metallicity estimates, we construct estimates of the global age and metallicity gradients

and intercepts (at the K band disc half-light radius), using an unweighted least-squares fit (c.f. BdJ). K band disc central surface brightnesses and scale lengths are determined by fitting the first 3 (gas) disc scale lengths of the surface brightness profile. Global gas fractions are determined by direct summation of the model gas and stellar masses.

The sample galaxies from BdJ cover a broad range of magnitudes and surface brightnesses. Therefore, to provide a fair comparison, the model galaxies must cover a similarly broad range of magnitudes and surface brightnesses. We adopt an empirical approach: we run a grid of 357 models with total (baryonic and dark) masses between 10^9 M_\odot and 10^{14} M_\odot (we assume a baryon fraction of 0.05 hereafter), and central baryonic surface densities between $10^{0.5} \text{ M}_\odot \text{ pc}^{-2}$ and $10^{4.5} \text{ M}_\odot \text{ pc}^{-2}$. The step size is 0.25 dex. This range is sufficient to cover the full observed range of parameter space probed in BdJ, assuming that the baryonic content of a galaxy turns entirely into solar-type stars.

However, this situation is complicated by the (broad) correlation between surface brightness and magnitude (c.f. Fig. 12 from BdJ, or the grey dots in panel a of Fig. 1). Because of this correlation between surface brightness and magnitude, any correlation between e.g. age and surface brightness will automatically translate into a correlation between age and magnitude. However, our model grid does not incorporate this correlation. Therefore, to provide a fair comparison with the data, we select galaxies from the model grid that fall within the region inhabited by the sample galaxies in the K band surface brightness–absolute magnitude plane (Fig. 1) using the following criteria:

$$\mu_{K,0} > 13 + 0.6(M_K + 26) \quad (5)$$

$$\mu_{K,0} < 20 + 0.6(M_K + 26) \quad (6)$$

$$\mu_{K,0} > 19 - 1.25(M_K + 28) \quad (7)$$

$$\mu_{K,0} < 23 - 1.25(M_K + 21), \quad (8)$$

where $\mu_{K,0}$ is the K band disc central surface brightness and M_K is the K band absolute magnitude of the galaxy. In this way, we can empirically select galaxies with a range of physical parameters consistent with those taken from BdJ. This approach ensures that the galaxies we produce automatically roughly satisfy the selection criteria of BdJ's sample. We make no attempt to derive the allowed range of surface brightnesses and scale lengths on the basis of the angular momentum of infalling gas (e.g. Dalcanton, Spergel & Summers 1997; Mo, Mao & White 1998).

Note that galaxies with different sets of surface densities and masses may be chosen, depending on the model details (especially on the efficiency with which stars are turned into gas). We show an example of the selection box in panel a of Fig. 1 for the fiducial closed box model discussed in the next section. We show the K band central surface brightness against the K band absolute magnitude of the data (in grey) and the fiducial model (in black). The model points show clearly the selection criteria that are applied on the model central surface brightnesses and magnitudes: these selection limits are applied to preserve the broad correlation between surface brightness and magnitude in the dataset, and to make sure we do not compare the data with models of galaxies that are drastically different from those in the data. Panel b of Fig. 1 shows the K band central surface brightness against gas fraction relation for the same fiducial

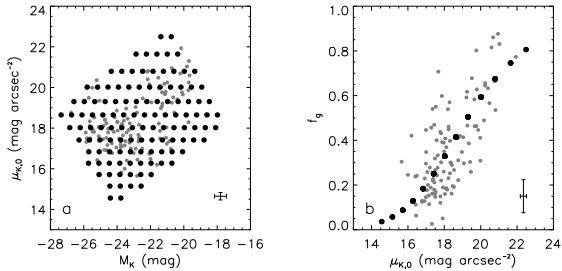


Figure 1. Fiducial Model: Correlation between K magnitudes and K band central surface brightnesses (panel a), and between K band central surface brightnesses and gas fractions (panel b). The data are from BdJ and are shown as grey circles (average error bars are in the bottom right corner of each plot) and the fiducial model is shown by black circles. Panel a shows our selection criteria based on the observed distribution of galaxies in the M_K vs. $\mu_{K,0}$ plane. Panel b shows the surface brightness–gas fraction correlation, which we use as a constraint when searching for adequate model fits to the data.

model. All of the models presented in this paper are constrained to reproduce this correlation (although, in the case of e.g. infall models, there is some scatter in this correlation).

Now we use this model grid to investigate trends in age and metallicity with local and global structural parameters in sections 3 through 5, where we vary the galaxy evolution and SFL prescriptions. A summary of the models presented in the following sections is given in Table 1. The age, stellar metallicity and gas metallicity gradients are also given for these models in Table 2: note that there may be some slight mismatch in the properties of the observed and model galaxies (e.g. in panel a of Fig. 1 the model galaxies are regularly distributed in a rectangle, whereas the observed galaxies are clustered primarily towards the centre with a fairly significant contingent of galaxies with more extreme properties) which may affect the comparison of the average model and observed gradients slightly.

2.4 How we compare the models and the data

In the subsequent sections, we compare the colour-based ages and metallicities of a sample of face-on spiral galaxies with colour-based ages and metallicities from a suite of simple galaxy evolution models. However, earlier we stated that the colour-based ages and metallicities were only robust in a *relative* sense. This leaves open an important issue: how should we approach the comparison of the model ages and metallicities and the data?

To understand how we should approach these model comparisons, we need to go back to understanding the nature of the data. In essence, the trends in the data of e.g. Fig. 2 are describing trends in colour with galaxy properties. Therefore, if the black model points describe well the trends in age or metallicity with galaxy properties, then what the model really does is adequately describe the trend in optical–near-IR colour with galaxy properties. The model, of course, has one significant limitation: it interprets the trends in colour solely in terms of smoothly varying SFHs under the

assumption of a constant IMF. The data, in contrast, has contributions to the colours from bursts of star formation, dust, and possibly from variations in the IMF.

Low-level bursts of star formation (e.g. variations of a factor of two in SFR over 0.5 Gyr timescales; Rocha-Pinto et al. 2000b) are relatively unimportant: these bursts only contribute modest extra scatter. IMF variations between different types of galaxy are disfavoured (see e.g. Kennicutt 1998; Bell & de Jong, in preparation). The overall IMF normalisation produces subtle effects, as the colours will change only very little for plausible changes in the IMF, but the galaxy evolution will be affected through e.g. the fraction of mass locked up in long-lived stars ($1 - R$). Therefore, IMF uncertainties are unlikely to affect the qualitative behaviour of our models but may require the adoption of e.g. slightly different SFL parameters such as n or k . Similar effects are expected for some types of model uncertainty or model age differences.

Dust is one major remaining uncertainty. The amounts and effects of dust are still hotly debated (Disney, Davies & Phillipps 1989; Peletier & Willner 1992; Huijzinga 1994; Tully et al. 1998; Kuchinski et al. 1998), so being quantitative about the effects of dust is difficult. The zeroth order expectation is that dust is unlikely to be important for e.g. low surface brightness or luminosity galaxies, and is much more important for higher luminosity or surface brightness galaxies (e.g. Tully et al. 1998). In this scenario, young and metal poor galaxies would be little affected by dust; however, the older and more metal-rich galaxies would be likely to appear even older and more metal-rich, if dust was properly accounted for.

For these reasons, it is not fair to take the details of the model comparisons with the data too seriously. However, the relative trends shown by the comparison should be reasonably robust and it is certainly fair to compare the performance of different models. Also, along the same vein, we compare the models on a qualitative, visual level because no simple statistical approach (e.g. a two dimensional Kolmogorov-Smirnov test or least-squares line fitting) can take into account both the modelling uncertainties that we have discussed above and the role of selection effects in limiting the area of parameter space that is observed. We show all of the relevant plots for each model so that the reader can make their own comparisons and assessments of the different models.

3 CLOSED BOX MODEL

Our fiducial model is a closed box model (i.e. $E = F = 0$ in equations 2 through 4) with a Schmidt SFL, with efficiency $k = 0.012 \text{ M}_\odot \text{ pc}^{-2} \text{ Gyr}^{-1}$ at a surface density of $1 \text{ M}_\odot \text{ pc}^{-2}$ and $n = 1.6$ (see Table 1; note that modest increases in n are possible if k decreases, and vice versa). The primary prediction of the closed box Schmidt SFL model is that *the SFH and metallicity of a given area in any galaxy depend only on the initial local gas surface density*. Note that the star formation and chemical enrichment history of a galaxy are *independent* of the initial density of gas if $n = 1$, i.e. if the star formation rate is directly proportional to the gas density.

When we evaluate the effects of different galaxy evo-

Table 1. Models presented in this paper

Model	SFL	n	k	Threshold	Yield	Chemical Evolution
Fiducial	Schmidt	1.6	0.012	-	0.02	closed box
I	Schmidt	1.8	0.012	-	0.02	galaxy mass and radius dependent infall
O	Schmidt	1.6	0.012	-	0.03	more outflow from smaller galaxies
E	Schmidt	1.7	0.012	-	0.03	mass dependent formation epoch
T	Schmidt	1.8	0.012	Y	0.02	infall case I
D	Ke98	1.0	0.030	-	0.02	closed box

lution prescriptions, we will evaluate them with respect to this model. As such, it is worth spending some time on understanding what this model can and cannot reproduce, in terms of the trends observed in BdJ.

In Fig. 1 we show the fiducial model selection box and K band central surface brightness–gas fraction correlation. As discussed in the last section, these two plots are used to select the galaxy models (panel a) and help to constrain the SFL parameters (panel b). In Fig. 2 we show the local age (panel a) and local metallicity (panel b) against the local K band surface brightness. These local ages, metallicities and surface brightnesses are for individual one scale length wide annuli in the sample and model galaxies: in the limit of a SFL that depends on gas density only (such as the Schmidt law), these correlations should be unique, well-defined lines with no intrinsic width (e.g. the black model points).

In panels a and b of Fig. 2 we see that the fiducial model does a good job of reproducing the observed trends in age and metallicity with local K band surface brightness. Although age and metallicity increase monotonically with surface brightness in the model, the ages (or metallicities) derived from the colours show more irregular trends with surface brightness. This is primarily due to degeneracies and irregularities in the colour-colour grid for stellar populations with near-constant star formation rates (i.e. average ages ~ 6 Gyr), which cause irregularities in the age–surface brightness and metallicity–surface brightness plots.

However, the observational data have significant scatter: while this is partly due to observational errors, there is a component of the scatter which is real intrinsic scatter in annulus colour at a given surface brightness. This indicates at least departures from a smooth SFH (e.g. Rocha-Pinto et al. 2000b), and potentially indicates dependence on some factor other than the local K band surface brightness (BdJ). Thus, while the model gives a good match to the overall trend, additional factors need to be introduced to account for the scatter between annuli with the same K band surface brightnesses.

Recall that we carried out linear fits to trends in age and metallicity with radius within a galaxy (yielding an intercept at the half-light radius and a gradient per K band disc scale length). In panels c and d of Fig. 2 we explore the correlations between the age intercept at the half-light radius and the K band central surface brightness (panel c) and absolute magnitude (panel d). We see that the fiducial model produces a correlation between the age at the half-light radius and the K band central surface brightness (panel c: also between age and gas fraction; not shown). Note however that the slope of the model correlation is too shallow: real galaxies show a steeper correlation between age at the

half-light radius and K band central surface brightness than the model galaxies.

The selection limits imposed on the model galaxies produce a small residual correlation between age at the half-light radius and K band absolute magnitude (panel d): this correlation is fictitious (age does not depend on mass in this model) and is the result of the magnitude–surface brightness correlation shown in panel a of Fig. 1. The correlation imposed by the magnitude–surface brightness correlation on panel d of Fig. 2 is too shallow compared to the data, however.

In panels e and f of Fig. 2 we explore correlations between the metallicity intercept at the disc half-light radius and the K band central surface brightness (panel e) and absolute magnitude (panel f). Note that the model grid becomes quite uncertain at low metallicities: many of the grey data points at metallicities lower than $\log_{10}(Z_{\text{eff}}/Z_{\odot}) = -1$ may not have metallicities as low as those plotted (BdJ). The metallicity–surface brightness correlation (panel e: and metallicity–gas fraction correlation; not shown) is well-described by the fiducial model. We can also see from panel f of Fig. 2 that there is a small residual correlation between metallicity and magnitude imposed by the selection limits in panel a of Fig. 1, but that the slope of the correlation is too small: this indicates that metallicity has both a surface brightness and magnitude dependence (see e.g. BdJ; Skillman, Kennicutt & Hodge 1989; Garnett et al. 1997).

In panels g and h of Fig. 2 and Table 2, we explore the age (panel g) and metallicity (panel h) gradients per K band disc scale length. Note that these gradients are considerably noisier than the intercepts that were discussed above: in particular, individual metallicity gradients are often only marginally detected (see BdJ for an indication of the uncertainties, and versions of these data plots with error bars).

Both the amplitude of and trends in age gradient with K band central surface brightness are poorly reproduced by the fiducial model (panel g of Fig. 2): there is little if any correlation between age gradient and surface brightness in the model, and the model underpredicts the average age gradient in the data by around a factor of two (see Table 2). This problem may be linked with the inability of the model to reproduce the steepness of the global age– K band central surface brightness correlation in panel c of Fig. 2, as the slope of the model correlation is too shallow, indicating that the rate of change of age with surface brightness (i.e. the age gradient) is underpredicted by the model. In contrast, the fiducial model reproduces both the average metallicity gradient and the trends in metallicity gradient with K band central surface brightness (albeit with no scatter in

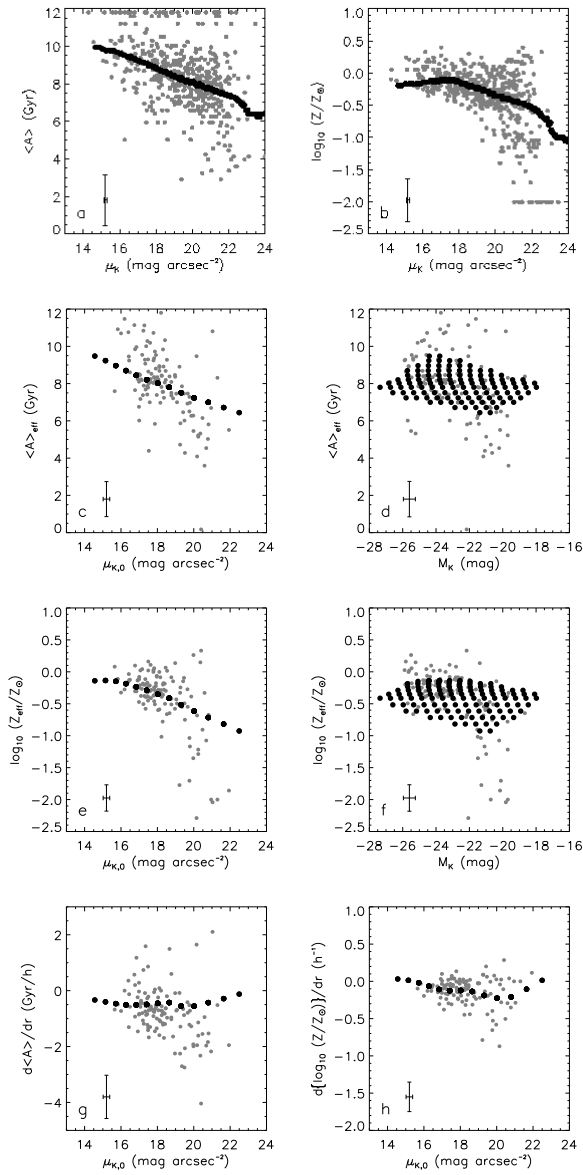


Figure 2. Fiducial Model: Panels a and b show the correlation between local K surface brightness and the local age (panel a) and metallicity (panel b) of the data from BdJ (grey circles; average error bars are in the bottom left corner) and the fiducial model (black circles). Panels c through f show correlations between the ages at the disc half-light radius and the K band disc central surface surface brightness $\mu_{K,0}$ (panel c) and the K band absolute magnitude M_K (panel d), and between the metallicity at the disc half-light radius and the K band disc central surface surface brightness (panel e) and the K band absolute magnitude (panel f). In panels g and h we show correlations between the age (panel g) and metallicity (panel h) gradients per K band disc scale length and the K band central surface brightness. In panels a and b, a significant number of the grey data points from BdJ have average ages of 11.9 Gyr or metallicities of $\log_{10}(Z/Z_{\odot}) = -2$: these data points fall outside the model grids. The model grid becomes quite uncertain at very low metallicities: many of the grey data points in panels b, e and f at metallicities lower than $\log_{10}(Z_{\text{eff}}/Z_{\odot}) = -1$ may not have metallicities as low as those plotted on this diagram. Some of the older, very low surface brightness galaxies may have significant age errors in panels c and d (Bell et al. 2000).

the model metallicity gradients; Table 2 and panel h of Fig. 2).

To summarise, the fiducial model does a reasonable job of describing the correlations between the ages and metallicities of galaxies and their physical parameters. The main shortcomings of the fiducial model are a lack of magnitude dependence in both the age and metallicity (panels d and f of Fig. 2) and the underprediction of the rate of change of age with K band surface brightness (Table 2 and panels c and g of Fig. 2). An additional shortcoming which we address more explicitly later in section 6 is that closed box models predict too many low metallicity stars in both the solar neighbourhood and in external galaxies (the G dwarf problem; e.g. Rocha-Pinto & Maciel 1996; Worthey, Dorman & Jones 1996; Pagel 1998). In the next section, we see how modifying the fiducial model by introducing infall, outflow or systematic trends in galaxy formation epoch can improve the match between the models and the observed correlations.

4 GALAXY EVOLUTION PRESCRIPTIONS

Can any of these shortcomings of the fiducial model be alleviated by invoking infall, outflow or variations in formation epoch between galaxies? Infall is a natural part of galaxy formation: at some level the disc of a spiral galaxy must be built up by infall, and a plausible explanation for the local G dwarf problem is an extended infall history at the solar cylinder (e.g. Tinsley & Larson 1978; Lacey & Fall 1983; Pagel 1998; Boissier & Prantzos 1999). Outflow is somewhat more speculative: successful hierarchical models of galaxy formation rely on negative feedback to suppress star formation in low-mass systems at early times. Without feedback, these models generically produce too many faint galaxies to be compatible with the observed luminosity function (e.g. Kauffmann & Charlot 1998; Somerville & Primack 1999; Cole et al. 2000). The most likely source of feedback is the energy released by Type II supernovae. The feedback may take several forms: e.g. it may result in the preferential ejection of high metallicity gas or it may result in a ‘super-wind’ which completely removes the gas content of the galaxy (e.g. Dekel & Silk 1986; Arimoto & Yoshii 1987; MacLow & Ferrera 1999; Martin 1999). Significant differences in formation epoch (i.e. significant differences in the time at which a galaxy’s gas supply becomes available for star formation) between galaxies of e.g. different masses or halo spin parameters are quite possible. Semi-analytic, linear collapse and gas-dynamical cosmological simulations all suggest systematic trends in galaxy formation epoch with halo properties (e.g. Cole et al. 2000; Mo, Mao & White 1998; Steinmetz & Müller 1995). We explore the effects of infall, outflow and variations in formation epoch below in the next three subsections.

4.1 Infall

In order to test the effects of infall, we adopt a simple parameterisation. We assume that the infall timescale varies with both galaxy mass and radius within a galaxy: a radial dependence, and to a certain extent, a mass dependence in infall timescale are expected theoretically (e.g. Eggen, Lynden-Bell & Sandage 1962; Larson 1976; Contardo et al.

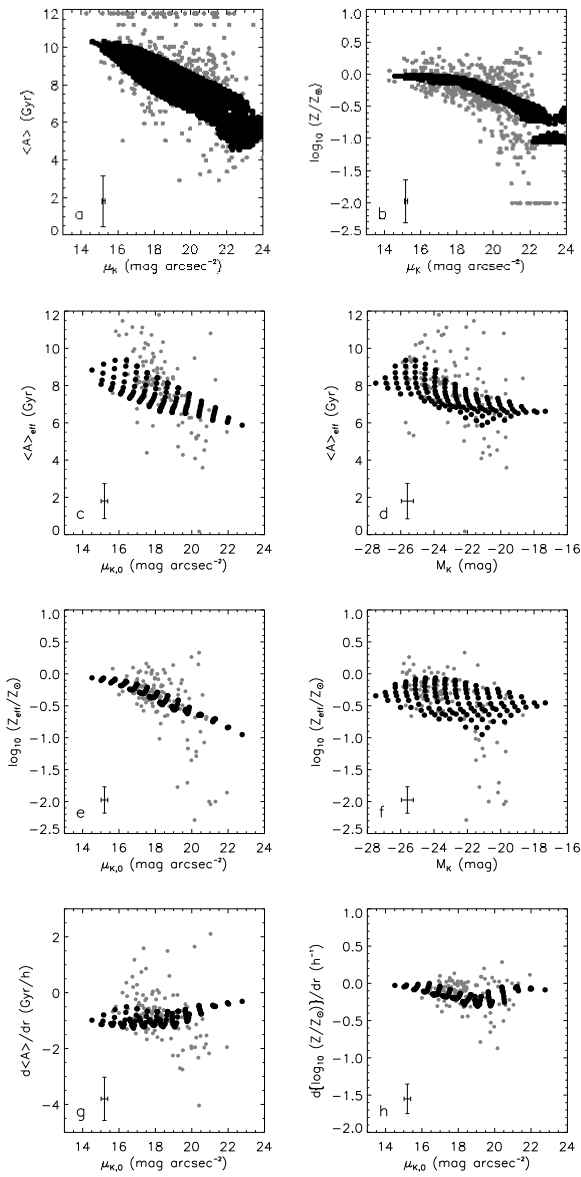


Figure 3. Infall Model I: Panels and symbols are as in Fig. 2

1998; Mo, Mao & White 1998; Boissier & Prantzos 2000; Cole et al. 2000). We have also run cases with only mass-dependent infall timescales, and even a mass-independent infall timescale; however, these cases are not discussed further as the effects of each of these individual cases are included (and are easily distinguished) in the infall model we consider.

We assume that the galaxy initially has a surface density of zero at all radii: we then build up the exponential disc of the galaxy from a reservoir of metal-free gas with an exponential timescale τ_{infall} . The infall timescale depends on both mass and radius. The timescale τ_{infall} ranges from $\tau_{\text{infall}} = 8$ Gyr for galaxies with a total mass of $10^{10} M_{\odot}$ to $\tau_{\text{infall}} = 0.5$ Gyr for galaxies with a total mass of $\geq 10^{13} M_{\odot}$ according to the formula: $\tau_{\text{infall}} = 8 - 2.5 \log_{10}(M_{\text{galaxy}}/10^{10} M_{\odot})$ for galaxies with masses lower than $M_{\text{galaxy}} = 10^{13} M_{\odot}$; for

galaxies more massive than $10^{13} M_{\odot}$ the infall timescale is fixed at 0.5 Gyr. Thus the most massive galaxies build up their gas mass quickly, and then evolve almost as a closed box, while low-mass galaxies have only recently reached their maximum gas mass and star formation rate. In this model, the infall starts at the same epoch in every galaxy and is always a decaying exponential: we investigate the effects of varying the formation epoch in Section 4.3.

The above infall timescales are defined at the half-light radius R_e . To impose radial variation, we reduce the central infall timescale by a factor of two and the infall timescale at $2R_e$ is doubled. As an example, a $10^{12} M_{\odot}$ galaxy in this model has infall timescales at $(0, 1, 2)R_e$ of $(1.5, 3, 6)$ Gyr.

All the model galaxies with infall have a Schmidt SFL with exponent $n = 1.8$ and efficiency $k = 0.012$. Note that these models have a different Schmidt law exponent from the fiducial model: this is because infall delays star formation compared to the closed box model, therefore star formation must be more efficient than in a closed box to provide a satisfactory match to the age observations.

From Fig. 3 (comparing it to Fig. 2 for the fiducial model) we can see that infall mainly affects the ages of the model galaxies. The reduction of the average age depends (of course) on the infall timescale: the maximum average age of a stellar population with an exponential infall timescale τ_{infall} decreases as the infall timescale increases (and is roughly $12 - \tau_{\text{infall}}$ Gyr for $\tau_{\text{infall}} \lesssim 4$ Gyr). Metallicity is affected less: the difference between the mean stellar metallicity of a closed box and an exponential infall timescale model at a given gas fraction (therefore roughly surface brightness) is $\lesssim 0.1$ dex for any plausible SFL. Infall does ‘narrow’ the metallicity distribution of a stellar population, where there are relatively less low and high metallicity stars than the closed box model: this in fact was one of the original motivations for the infall model (e.g. Larson 1972; Tinsley 1980; Prantzos & Aubert 1995; Pagel 1998; Prantzos & Silk 1998).

The mass dependence in the infall timescale introduces a slope in the magnitude–age intercept relation (panel d in Fig. 3). The slope is too shallow to adequately describe the trends in the data; however, this is closely linked to the underprediction of the slope of the age intercept–central surface brightness correlation (panel c in Fig. 3) which feeds into a shallow slope for the age intercept–magnitude correlation. Tuning a better match with an infall model is difficult: the real problem is achieving a stronger variation of age with surface brightness which is still consistent with the data in panels a and c of Fig. 2. Perhaps this could be linked to a central surface density dependent infall history (e.g. through a spin parameter dependence in halo formation timescale); however, adding yet another parameter to the infall model is unappealing both in terms of the simplicity of the modelling technique and the quality of the data at this stage.

The radial dependence in the infall timescale increases the age gradient: this is illustrated in panel g of Fig. 3 and Table 2, where the metallicity gradients (both gas and stellar) are relatively unchanged from the closed box case, but the age gradient is increased by a factor of two. Both the radial and mass dependence increases the scatter in the local age–local K band surface brightness relation, but not towards unacceptable levels.

To summarise: infall affects primarily the age of a re-

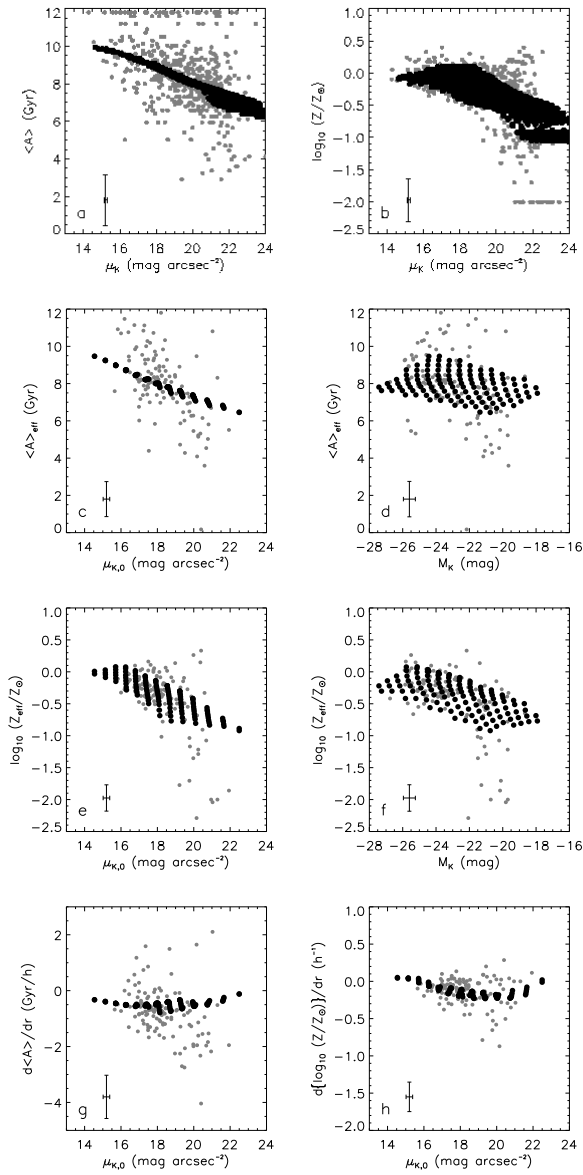


Figure 4. Outflow Model O: Panels and symbols are as in Fig. 2

gion within a galaxy, but does not significantly affect the mean metallicity of the stellar population. Therefore, mass (or radial) variation of the infall timescale introduces mass dependence (or a radial gradient) in the age of a galaxy.

4.2 Outflow

In order to test the possible importance of outflow, we adopt a basic parameterisation of its effects. Outflow caused by supernovae winds is predicted to be much more effective for low-mass galaxies (Dekel & Silk 1986; Arimoto & Yoshii 1987; MacLow & Ferrera 1999; Martin 1999; Cole et al. 2000). Furthermore, for galaxies with total masses in excess of $10^9 M_\odot$, there may be little gas mass loss; however, many of the freshly-synthesized metals can be lost reason-

ably easily (MacLow & Ferrera 1999). Accordingly, we adopt this simple outflow recipe: galaxies with masses greater than $10^{13} M_\odot$ lose no metals in an outflow; galaxies with masses lower than $10^{13} M_\odot$ lose increasingly more and more metals with decreasing mass, down to a limit of $10^9 M_\odot$, where a galaxy loses 90 per cent of its freshly-synthesized metal content. *We assume negligible gas mass loss in the outflow* in order to separate the effects of outflow from those discussed in the previous section: the fraction f of metal mass is given by $f = 0.9 - 0.225 \log_{10}(M_{\text{galaxy}}/10^9 M_\odot)$ below $M_{\text{galaxy}} = 10^{13} M_\odot$; for $M_{\text{galaxy}} \geq 10^{13} M_\odot$ we assume no metal-enriched outflow. This approximation glosses over all the physics behind outflow; however, it does allow us to explore the possible effects of outflow in a simple, well-defined way. Note that there is no infall in this model.

Results from the outflow model (model O) are shown in Fig. 4. Note that we have increased the true yield p from solar metallicity for the fiducial model to 1.5 solar metallicity for the outflow case: as outflow involves the loss of metals from the model galaxies, a larger yield must be used to allow the models to reproduce the mean observed metallicities. In contrast with the infall case, outflow leaves the colour-based age of a stellar population relatively unaffected. This is to be expected since the SFL only depends on gas density and since there is no gas *mass* loss in the outflow, the SFHs of the outflow model are the same as those from the closed box fiducial model. However, outflow profoundly affects the metallicity of a galaxy, causing a great deal of scatter in the metallicity–local K band surface brightness diagram. The effects of outflow are visible in panels e and f of Fig. 4, where we plot the metallicity at the disc half-light radius against the galaxy parameters. Comparison of panels e and f of Fig. 4 for the outflow model with Fig. 2 for the fiducial (closed box) model clearly shows that outflow of this type produces a strong mass dependence in the galaxy metallicity; furthermore, a simple model of this type reproduces the metallicity scatter fairly accurately.

To summarise: outflow affects the metallicity of a galaxy. If outflow is mass dependent, it can imprint a metallicity–mass correlation without significantly affecting the age of the model galaxies.

4.3 Variation in Formation Epoch

In the previous three models we have assumed that all galaxies start forming stars at a common epoch. Hierarchical models of galaxy formation predict that more massive galaxies, despite being *assembled* later (from a number of smaller subunits), have the bulk of their stellar population forming earlier than less massive galaxies (e.g. Somerville & Primack 1999; Cole et al. 2000). Furthermore, stripped-down linear collapse models (e.g. Mo, Mao & White 1998; Dalcanton et al. 1997) as well as the more comprehensive gas-dynamical simulations (e.g. Steinmetz & Müller 1995; Contardo et al. 1998) predict that disc formation must happen relatively late to produce disc galaxies that have anywhere near enough angular momentum to match the observations (although note that gas dynamical cosmological simulations produce discs that are typically too small to match the observations, e.g. Navarro & Steinmetz 1997; 2000). However, we have assumed in the previous sections that all galaxies are formed at a look-back time of 12 Gyr.

To investigate the impact of variations in the formation epoch ^{*} on spiral galaxy colours, we allow the formation epoch of a galaxy to depend on its halo mass, where galaxies with masses greater than $10^{13} M_{\odot}$ have formed at a look-back time of 12 Gyr, and galaxies with masses lower than $10^{13} M_{\odot}$ have formation epochs, E , smoothly decreasing from 12 Gyr at $M_{galaxy} = 10^{13} M_{\odot}$ to 4 Gyr at $10^9 M_{\odot}$ according to the formula $E(\text{Gyr}) = 4 + 2 \log_{10}(M_{galaxy}/10^9 M_{\odot})$. This approximation, in the spirit of this semi-empirical modelling, glosses over the important physics behind these variations in formation epoch in an attempt to gain insight into their most important observable consequences. We always assume a galaxy formation epoch of 12 Gyr when interpreting the broad band colours in the age and metallicity fitting routine. This assumption is necessary: it was the assumption used to derive the observational ages and metallicities, and in the fitting routine we have no *a priori* knowledge of the formation epoch of galaxies. An additional benefit of this modelling is to demonstrate how much effect different galaxy formation epochs would have on the observational ages and metallicities that we derive using this fitting routine.

The variable formation epoch galaxies are assumed to be closed box systems, with a yield of 0.03 (1.5 times solar) and Schmidt SFL exponent of $n = 1.7$ and efficiency at 1 $M_{\odot} \text{ pc}^{-2}$ of $k = 0.012 M_{\odot} \text{ pc}^{-2} \text{ Gyr}^{-1}$. The Schmidt SFL exponent was raised to 1.7 and the yield was increased to 0.03 to allow the rather younger galaxies reach gas fractions and metallicities at a given surface brightness which are in rough agreement with the observations. If the same set of Schmidt SFL model parameters were used as for the fiducial model the conclusions would be unchanged but the match to the observations would appear slightly poorer. No infall or outflow is included in this set of models.

One important caveat: we parameterise the formation epoch model by simply starting the evolution of the galactic disc at a particular look-back time. In practice, it might be more suitable to think of this model as allowing large amounts of very late infall. For example, if a small fraction of stars were formed at early times but the bulk of stars were formed only a few Gyr ago or less, we still parameterise that galaxy by a single, relatively recent formation epoch. The basic point is that the formation epoch really parameterises when the bulk of the gas supply became available for star formation: how that gas supply became available is relatively unimportant from this perspective.

We show the effects of the mass-dependent formation epoch in Fig. 5. One important first result is that because our colour-based age estimator is essentially a birthrate parameter estimator (estimating the proportion of young to old stars), it is possible to have large apparent galaxy ages for galaxies which are, in fact, relatively young. As an example, it is possible to get colour-based ages in excess of 9 Gyr in a galaxy which is only 4 Gyr old. The important message is that the age derived using this technique is not to be taken as a literal stellar population age; it is simply a

^{*} We reserve the term ‘formation epoch’ to indicate the look-back time at which stars start to form. We use the term ‘colour age’ (or simply ‘age’) to mean the average age of the stellar population as recovered from our colour inversion algorithm.

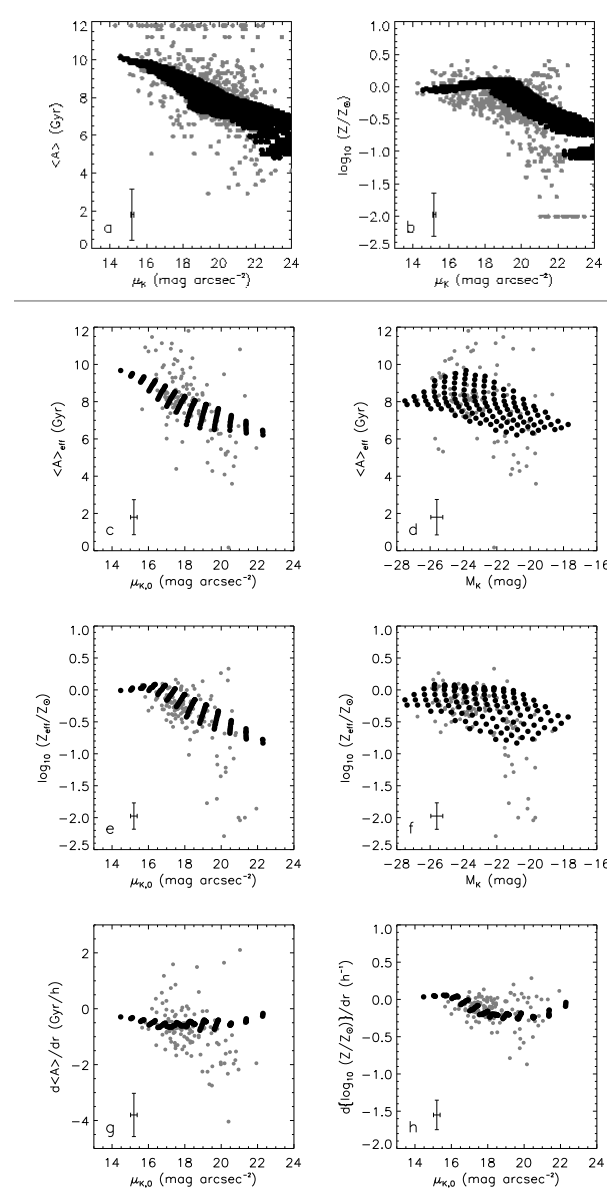


Figure 5. Formation Epoch Model E: Panels and symbols are as in Fig. 2

way of parameterising how the recent SFR compares to the SFR several Gyr ago.

We can see from Fig. 5, by comparison with the analogous figures for the closed box, infall and outflow models (Figs. 2, 3 and 4 respectively) that mass-dependent formation epoch variations between galaxies affects their ages and metallicities in ways similar to mass-dependent infall and outflow. In particular, formation epoch differences generate magnitude–age and magnitude–metallicity correlations that the fiducial model lacks.

4.4 Summary

To summarise:

- A local gas surface density-dependent Schmidt SFL describes many of the age and metallicity trends from BdJ surprisingly well. However, the slope of the age–central surface brightness correlation and the age gradients are underpredicted by the fiducial model.

- If the decay timescale of infall is mass-dependent, it can ‘imprint’ mass-dependency on the galaxy ages without significantly affecting their metallicities.

- If the infall timescale depends on radius, an age gradient can be generated without significantly affecting the metallicity gradient.

- If outflow is mass-dependent, it can ‘imprint’ a metallicity–mass correlation without significantly affecting the ages of the model galaxies.

- Variations in galaxy formation epoch do not invalidate our conclusion that a local surface density-dependent SFL describes the data reasonably well. However, mass-dependent variations imprint an age–magnitude and metallicity–magnitude relation even if no infall or outflow occurs.

In this way, the lack of mass dependence in the fiducial model may be provided *either* by mass dependence in the formation epochs of galaxies (where less massive galaxies are younger), *or* through a combination of mass dependent infall (where less massive galaxies have longer infall timescales) and outflow (where less massive galaxies lose a larger fraction of their newly-synthesized metal content). Furthermore, an ‘inside-out’ formation scenario may be able to reproduce the rather steep observed age gradients within individual galaxies.

We are therefore left in an uncomfortable situation: is there any way that we can differentiate between the effects of formation epoch variations versus infall and outflow? One possible approach is to study the *effective yield* of galaxies (i.e., the yield of a closed box model which reproduces the observed metallicity of a galaxy at its observed gas fraction). If the mass–metallicity correlation is due to mass-dependent variations in formation epoch then the effective yield should be constant. If, however, the mass–metallicity correlation is generated by mass-dependent metal-enriched outflows then the effective yield should strongly vary with galaxy mass, providing an observational test between the two possibilities.

We show the result of this experiment in Fig. 6 for the outflow and formation epoch models respectively. One can see that our naive expectation outlined above is confirmed: the outflow model (panel a of Fig. 6) has a strongly mass-dependent effective yield, whereas the formation epoch model has an almost constant colour-based effective yield (panel b of Fig. 6). The data do not clearly support either option: the effective yield of the faint, metal-poor galaxies denoted by crosses in Fig. 6 may be substantially underestimated due to stellar population model uncertainties at metallicities below 1/10 solar. However, if trend indicated by these points is correct, the colour-based effective yields marginally support the outflow model, although discounting the formation epoch model on data with this much uncertainty and scatter is clearly premature.

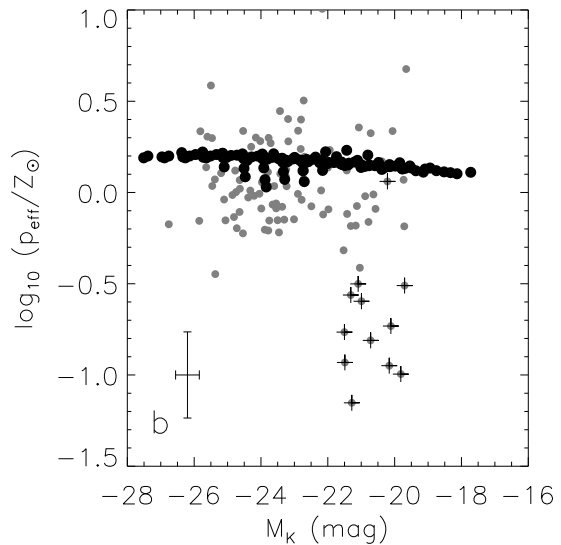
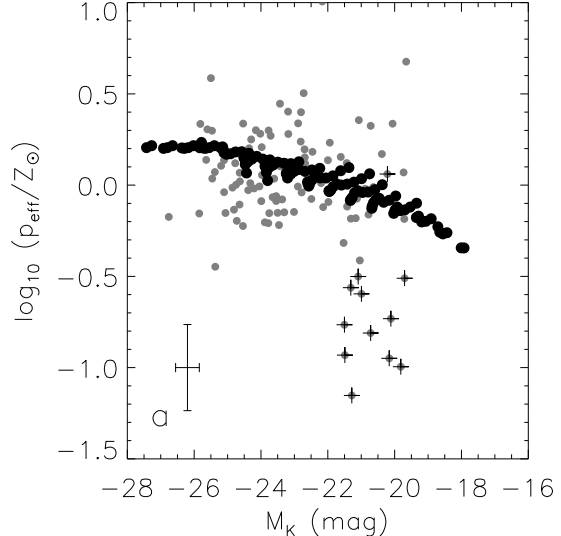


Figure 6. Panel a: **Outflow Model O.**, Panel b: **Formation Epoch Model E.** The colour-based effective yield (see text for a brief definition) of our sample galaxies against K band magnitude for the galaxies from BdJ (grey circles) and the model (black circles). Crosses denote data points with colour-based metallicities less than 1/10 solar: these points may have substantially underestimated metallicities due to model uncertainties and thus substantially underestimated effective yields (Bell et al. 2000; BdJ). The error bar denotes the average error, taking account of metallicity and gas fraction uncertainties.

5 STAR FORMATION LAWS

We have not yet considered changes in the SFL: as we found that our results were quite sensitively affected by the SFL in the Schmidt law model, it is worth investigating if some of the shortcomings of the fiducial model can be alleviated by the use of an alternative SFL.

Table 2. Model gradients

Model	Gradients		
	Age Gyr/h	Stellar met. dex/h	Gas met. dex/h
Fiducial	-0.47	-0.13	-0.18
I	-0.89	-0.16	-0.22
O	-0.48	-0.13	-0.18
E	-0.52	-0.14	-0.19
T	-1.02	-0.16	-0.22
D	-0.85	-0.14	-0.37
Observations	-0.78	-0.13	-0.20

Model gradients are averages over all selected galaxies (see the selection criteria in Fig. 1 and section 2.3) and the observed gradients are averages over the observational sample of BdJ (for age and stellar metallicity gradients) and the sample of Garnett et al. 1997 for the gas metallicity gradients.

5.1 Density threshold

One possible modification to the star formation law is the imposition of a cutoff critical density Σ_c below which star formation cannot occur. Kennicutt (1989) found that the radially-averaged star formation rate (SFR) in a sample of 15 well-studied spiral galaxies was well-described by a critical density model. One physically motivated choice for that critical density is the maximum stable surface density of a thin isothermal gas disc, given by (Toomre 1964; Kennicutt 1989):

$$\Sigma_c = \alpha \frac{\kappa c}{3.36G}, \quad (9)$$

where α is a dimensionless constant of order unity, c is the velocity dispersion of the gas (which we take, as Kennicutt did, to be a constant $c = 6 \text{ km s}^{-1}$ for all galaxies) and κ is the epicyclic frequency (Kennicutt 1989). Kennicutt found that $\alpha \sim 0.67$ was a good fit to his data: stars typically did not form in regions where the density was lower than the critical density, and formed according to a Schmidt law with index $n \sim 1.3 \pm 0.3$ above the critical density threshold.

In order to estimate Σ_c for our model galaxies, we must assume a rotation curve: for simplicity, we adopt an adaptation of the mass-dependent ‘universal rotation curve’ from Persic & Salucci (1991) (where we adopt a baryonic mass of $1.5 \times 10^{11} M_\odot$ for a L^* galaxy with B band absolute magnitude of ~ -20.6 assuming $H_0 = 65 \text{ km s}^{-1} \text{ Mpc}^{-1}$). We use this rotation curve to determine the critical density in our model galaxies: we allow stars to form according to a Schmidt law with $n = 1.8$ and $k = 0.012$ in gas denser than the critical density and do not allow stars to form at densities lower than the critical density. *We do not use a critical density threshold in the central half scale length of the galaxy:* apart from the undoubtedly influence of bars and bulges in the central regions of galaxies (which we do not include in this model), the universal rotation curve is undefined in the inner regions of a galaxy, and the critical density becomes very large in the innermost regions of spiral galaxies due to strong differential rotation. Thus, the behaviour of this star formation law at small radii is ill-constrained in this model: we, therefore, neglect the existence of a critical density at small radii and form stars according to a Schmidt law.

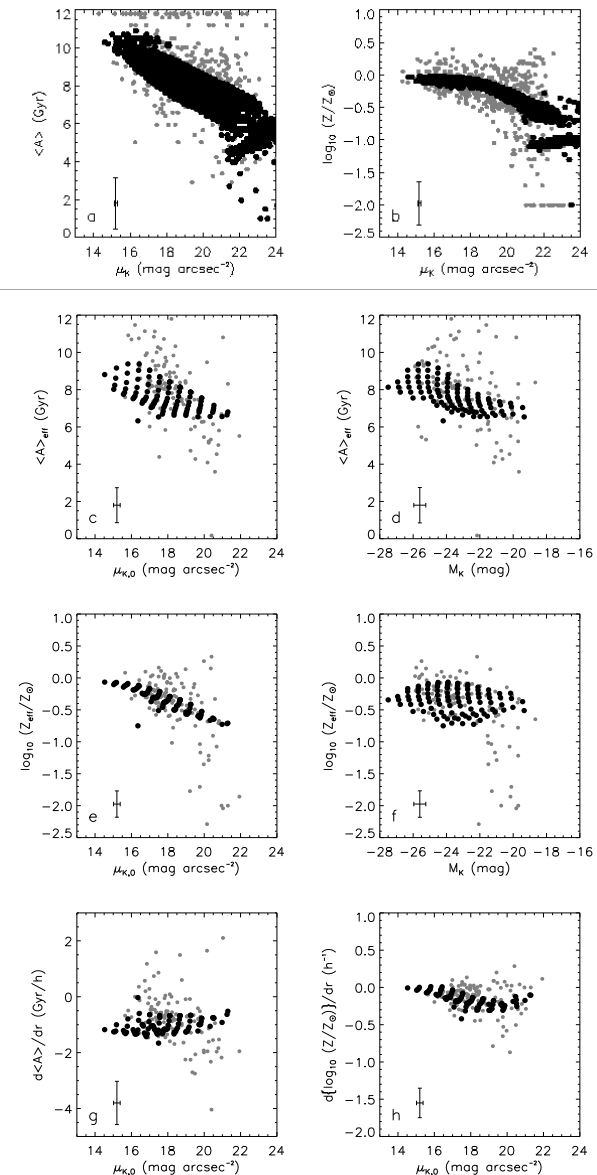


Figure 7. Critical Density with Infall Model T: Panels and symbols are as in Fig. 2

In Fig. 7 we show the ages and metallicities for a model with a critical density for star formation in which we adopt infall (see section 4.1). Comparison with Fig. 3 (and inspection of Table 2) shows that the imposition of a critical density does little to affect the colour-based ages or metallicities of spiral galaxies. Only regions with relatively low gas densities are affected significantly: regions near the centre of galaxies where the gas is depleted by star formation may be affected (although note that we do not impose the critical density within the central half scale length of our model galaxies), and the outermost regions where infall only recently brought the gas density above the critical density. In these outer regions the ages can be somewhat younger than those of the infall model without a critical density (compare

the colour-based ages of those regions with the lowest K band surface brightnesses in panel a of Figs. 7 and 3).

To summarise: the critical density threshold proposed by Kennicutt (1989) does little to affect the global correlations between SFH and physical parameters predicted by models with a Schmidt SFL. This is not to say that the existence of a critical density threshold has no effects at all: it is merely to state that the existence of a critical density threshold for star formation mainly affects the spatial distribution of present day star formation and does little to affect the star formation or chemical enrichment histories as probed by our colour-based technique.

5.2 Dynamical time dependence

An alternative SFL was proposed by Kennicutt (1998; Ke98 hereafter) based on his analysis of the global SFRs of a large sample of spiral and starburst galaxies. The SFR in this case scales with the ratio of the gas density to the local dynamical timescale:

$$\psi = k\Sigma_{\text{gas}}/\tau_{\text{dyn}}, \quad (10)$$

where $\tau_{\text{dyn}} = 6.16R(\text{kpc})/V(\text{km s}^{-1})$ Gyr is the dynamical timescale, here defined as the time taken to orbit the galaxy at a distance R . In this picture, the SFR is related to both the gas supply and the timescale in which the gas can be brought together. As we did for the critical density model, we use the mass-dependent universal rotation curve of Persic & Salucci (1991) to estimate the dynamical time as a function of radius in our model galaxies. This SFL is similar in many ways to the radially-dependent SFLs proposed by Wyse & Silk (1989) and allows us to explore how explicit radial dependence in the SFL affects how we interpret the trends in SFH with galaxy parameters presented in BdJ.

In Fig. 8 we show the ages and metallicities given by the dynamical time model (Model D) overplotted on the data from BdJ. The dynamical time dependence does three main things: it introduces significant (but reasonable) scatter in the local ages and metallicities, it produces anticorrelations between age/metallicity and magnitude, and it produces steeper age and gas metallicity gradients. The production of relatively steep age and metallicity gradients is a success of this type of model. Steep age gradients are expected from this model: in the limit of a flat rotation curve the Ke98 SFL depends linearly on gas density, and the star formation efficiency varies as $1/R$, leading to larger star formation timescales at larger radii. However, the observed *trend* in age gradient with surface brightness is not reproduced by the dynamical time model (or, indeed, the infall model): in both the dynamical time and infall model the age gradients are steeper for higher surface brightness galaxies, which is the opposite of the observed trend (Fig. 2).

Another more serious shortcoming of this model is the production of a ‘backwards’ age–magnitude and metallicity–magnitude correlation. This is at first sight counter-intuitive: brighter galaxies have larger rotation velocities, which would increase the SFR at a given gas mass and physical radius. However, brighter galaxies are also typically larger, therefore there is little change in the average ratio of radius to velocity, that is, there is little change in the typical dynamical time as a function of magnitude. There is obviously a scatter in these properties, leading to a scatter in

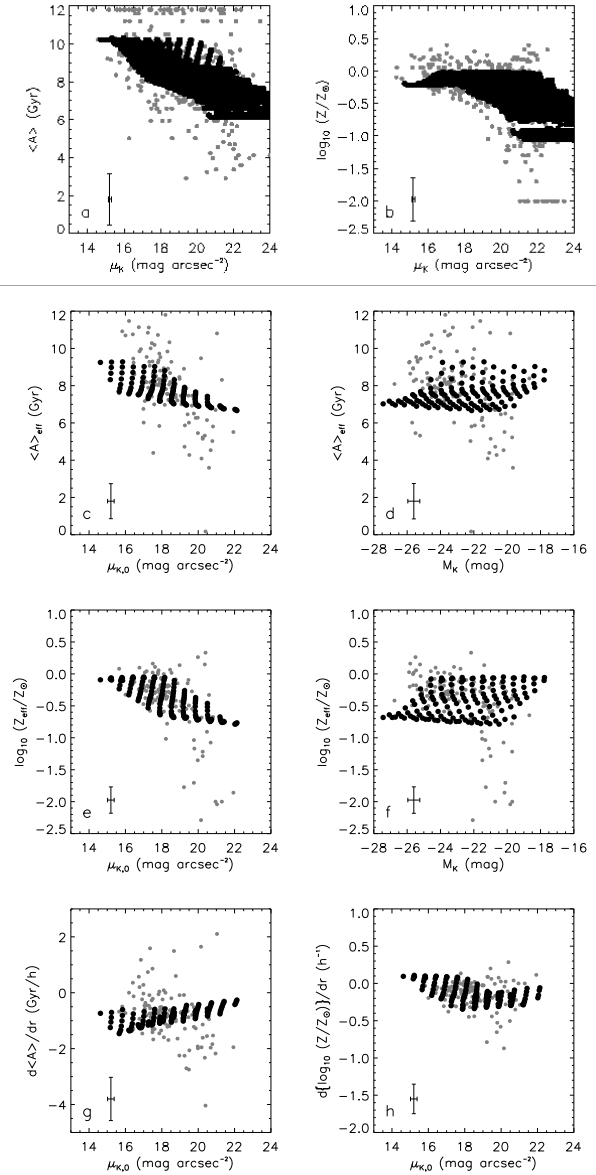


Figure 8. Dynamical Time Model D: Panels and symbols are as in Fig. 2

SFHs. The ‘backwards’ age/metallicity–magnitude correlation is generated by the correlation between magnitude and surface brightness: small galaxies have older stellar populations in this model, and the smallest galaxies are also the faintest galaxies (see Fig. 1).

To summarise: the dynamical time model, due to its explicitly radius-dependent SFR, generates steeper age and metallicity gradients, compared to the fiducial closed box model. However, the dynamical time, on average, does not significantly depend on magnitude. Coupled with the surface brightness–magnitude correlation, this implies that the faintest galaxies appear, on average, older than the brightest galaxies, which is clearly at odds with the observations. Therefore a dynamical time dependence, alone, is not favoured by our dataset.

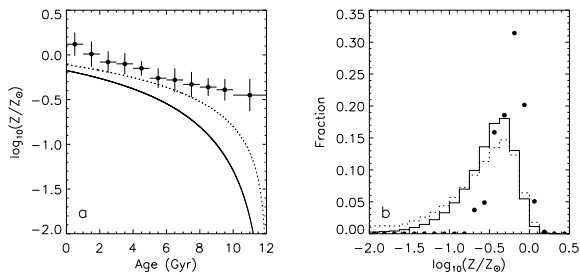


Figure 9. A comparison of the age-metallicity relation (panel a; points with error bars are from Rocha-Pinto et al. 2000a) and the oxygen metallicity distribution (panel b; solid dots are from Rocha-Pinto & Maciel 1996 converted into oxygen abundance following Edvardsson et al. 1993) of the solar circle with the model predictions for the infall model I (solid lines) and closed box fiducial model (dotted lines).

6 DISCUSSION

In contrast to the previous sections, where we tuned the models to improve the match with the observational data, in this section we discuss three ‘blind’ applications of the models to literature data: the models were not tuned to fit these observations (solar cylinder data, global SFRs and gas metallicities), and they represent a powerful test of the model’s validity. We also present a comparison of our models and the model of Boissier & Prantzos (2000).

6.1 Properties of the Milky Way

Many chemical evolution models focus (sometimes almost exclusively) on the Milky Way (e.g. Wyse & Silk 1989; Steinmetz & Müller 1994; Prantzos & Aubert 1995; Boissier & Prantzos 1999; Portinari & Chiosi 1999): only after the models have been normalised to the Milky Way are the models extended to external galaxies, if at all (e.g. Wyse & Silk 1989; Boissier & Prantzos 2000; Prantzos & Boissier 2000). We have approached the problem from the other direction: we use the trends in galaxy properties with e.g. surface brightness or magnitude to learn what processes might be at play in determining the star formation and chemical evolution histories of galaxies. Nonetheless, it is interesting to check our models against observations of the ages and metallicities of stars in the solar cylinder, to provide a consistency check for our models.

In order to compare our models with the solar cylinder age and metallicity distributions, it is necessary to choose one model galaxy as a ‘Milky Way’. We choose to adopt a galaxy with a magnitude of around $M_K^* \sim -24$ and a K band disc scale length of around 2.5 kpc in the closed box model (this model galaxy has total mass of $10^{12} M_\odot$ and a baryonic central surface density of $1000 M_\odot \text{ pc}^{-2}$). In Fig. 9 (panel a) we show the solar cylinder age-metallicity relation (points and error bars; Rocha-Pinto et al. 2000a) against the model predictions at a galactocentric radius of 8.5 kpc for the fiducial model (dotted lines) and the infall model I2 (solid lines). Note that stars from Rocha-Pinto et al. (2000a) older than 10 Gyr and younger than 15 Gyr

have been put in a single bin centred at 11 ± 1 Gyr. In panel b of Fig. 9 we show the metallicity (taken to be the oxygen abundance; determined from their iron abundance by applying the trend in $[\text{O}/\text{Fe}]$ with iron abundance from Edvardsson et al. 1993) distribution of solar cylinder G stars taken from Rocha-Pinto & Maciel (1996) against the model distributions convolved with a gaussian of width 0.13 dex (to simulate the intrinsic metallicity spread of stars at a given age; Twarog 1980; Rocha-Pinto et al. 2000a).

From Fig. 9, we see that the models have some difficulties in reproducing the properties of the solar cylinder. Panel b of Fig. 9 clearly demonstrates that both our closed box and infall models have a significant G dwarf problem. This was expected: infall models require large amounts of late infall to solve the G dwarf problem (e.g. Pagel 1998). Possible solutions of this problem include pre-enrichment of the infalling gas from bulge and/or population III stars, more late infall, or some mixing of metals produced in outflows with the infalling gas. These additions are more complex processes that clearly need to be added to fine-tune the models. However, since any of the models could be tuned (in a few ways) to solve the galactic G dwarf problem, this problem does not in itself help us choose between models, and so these processes are not considered here for simplicity. The model age–metallicity relations are also not a perfect match to the data: our model age–metallicity relations are offset to lower metallicities, and show a steeper slope than the observed age–metallicity relation. While some of the slope mismatch may be due to the effects of observational errors (Rocha-Pinto et al. 2000a), the mismatches in the age–metallicity relation are related to the G dwarf problem: the model metallicity is always lower than the observations, especially so at early times.

The Milky Way analogue model gas metallicity gradient is $-0.055 \text{ dex kpc}^{-1}$, which is broadly consistent with observational estimates of between -0.05 and $-0.1 \text{ dex kpc}^{-1}$ (e.g. Vilchez & Esteban 1996; Smartt & Rolleston 1997; Pagel 1998). We therefore conclude that the models are a reasonable match to the observed ages and metallicities of solar cylinder stars, modulo a G dwarf problem, and that our approach of normalising the models on external galaxies has not seriously compromised the comparison with the Milky Way’s properties.

6.2 Comparison with the global star formation laws

Another important test is the comparison of the SFLs that we used in these models against observed SFRs. Here, we compare our fiducial Schmidt law model and the dynamical time model with observations of the globally averaged SFRs, gas densities and dynamical times of Ke98’s subsample of spiral galaxies. To make the comparison fair, we construct gas densities and SFRs averaged within the model galaxy’s R_{25} (i.e. interior to the $25 B$ mag arcsec^{-2} isophote), and we take the dynamical time at R_{25} .

This comparison is presented in Figs. 10 and 11 for the fiducial model and dynamical time model respectively. The left-hand panels show the globally averaged SFR as a function of the gas density, and the right-hand panels show the globally averaged SFR as a function of the average gas density divided by the dynamical time. The data are denoted

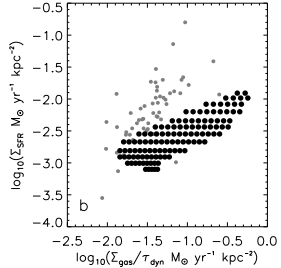
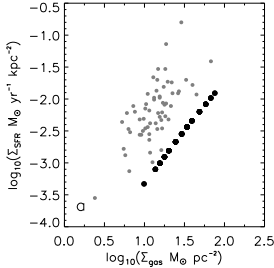


Figure 10. Fiducial Model: A comparison of the gas density and the star formation density interior to R_{25} (left) and the dynamical time SFR against star formation density interior to R_{25} (right). The data (grey points) are spiral galaxies taken from Ke98 and the SFRs from the fiducial model are denoted by black circles.

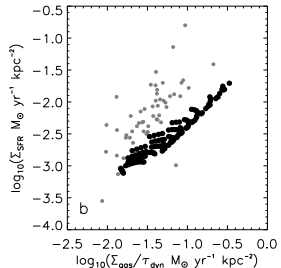
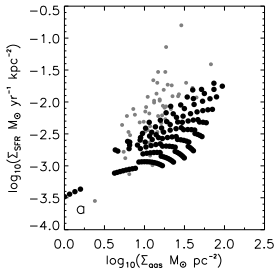


Figure 11. Dynamical Time Model D: Panels and symbols are as in Fig. 10.

by grey circles and the models by black circles. We can see that both models provide a fair match to the slope of Ke98's observations, and encompass the range of SFRs and gas densities typical of spiral galaxies. However, there is a significant zero-point offset between the model and the observations. A possible source of the zero-point offset is the efficiency of the SFL k : our model efficiencies are somewhat lower than e.g. those efficiencies used by Boissier & Prantzos (1999,2000). (Somewhat higher star formation efficiencies would be required to match the observations if we assumed younger galaxy ages or postulated large amounts of late gas infall as Boissier & Prantzos assume.) A higher efficiency raises the SFR at a given gas density, providing a better match to the observations. However, there are other possibilities: it is possible that there are aperture mismatches or discrepancies between the observational and model SFR calibrations (e.g. in the conversion of the $\text{H}\alpha$ flux to SFR).

6.3 Comparison with gas metallicities

Earlier, we compared the models to the colour-based stellar ages and metallicities of the sample of galaxies from BdJ. However, those ages and metallicities are subject to systematic errors from e.g. model uncertainties and dust reddening. For this reason, it is important to check the models against the *gas metallicities* derived from H II region spectroscopy

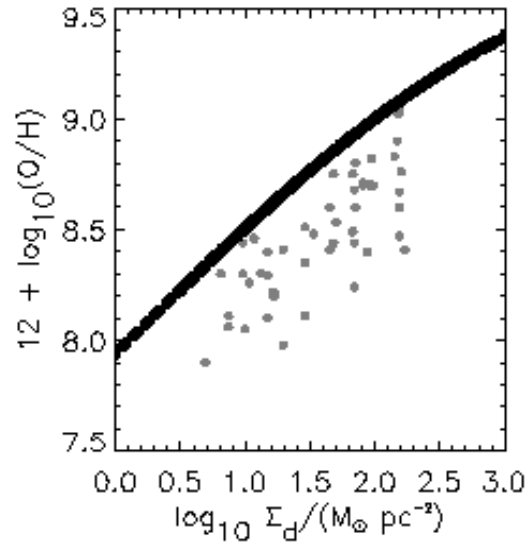


Figure 12. Fiducial Model: Comparison of trends in local gas oxygen abundance with baryonic surface density with the fiducial model predictions. The data are taken from Fig. 12 of Garnett et al. 1997 (grey dots; for M33 and NGC 2403 with B absolute magnitudes ~ -18.5), and the fiducial model predictions are overplotted as black circles.

of spiral galaxies: these metallicities are subject to a completely independent set of uncertainties, and as such offer a chance to check our models.

We have chosen to compare our model gas metallicities with data from Garnett et al. (1997) in Fig. 12, where we show the surface density–local gas metallicity correlation for M33 and NGC 2403 from their Fig. 12. Data from Garnett et al. (1997) are denoted by grey dots and the fiducial model output is shown as black circles. The model metallicity–surface density correlation has the right slope but an offset zero point.

That the closed box fiducial model reproduces the right slope of the metallicity–surface density correlation disagrees with the conclusions of Phillipps & Edmunds (1991), who concluded that observed metallicity gradients exceed those achievable with a Schmidt SFL and closed box chemical evolution. However, inspection of their Figs. 1 and 2 suggests a good agreement between their simple Schmidt law model and the observations, indicating that they may have overestimated the size of the observational trend between metallicity and surface density when compared to the Schmidt law model.

The offset zero point is a well-known problem: when simple models are used to infer a yield from observations of the oxygen abundances of spiral galaxies, the yield is estimated to be around 1/3 solar (e.g. Garnett et al. 1997; Pagel 1998). However, we require a yield of around or somewhat above solar to match the observations: this discrepancy amounts to an offset of around 0.5 dex, which is of the order of the offset between the average metallicity of the models and the observations. This discrepancy between the yield es-

timates indicates a mismatch between the colour-based and gas metallicities, although it is as yet uncertain whether this is a deficiency in the calibration of the colour-based metallicities, gas metallicities, or even both. However, uncertainties in the stellar mass-to-light ratios used to derive the surface densities will propagate into this comparison. In addition, M33 and NGC 2403 are relatively faint ($M_B \sim -18.5$), and because of the metallicity-magnitude correlation they are expected to have a somewhat lower metallicity than that of the fiducial model.

We do not show the comparison with their global gas metallicities here: the results are consistent with the overall yield offset between the gas and stellar metallicities outlined above and, again, the well-known gas metallicity-magnitude correlation (e.g. Skillman et al. 1989; Garnett et al. 1997) can only be adequately reproduced by the outflow or formation epoch model (as we found for the stellar metallicity-magnitude correlation). The average gas metallicity gradients of the model galaxies are presented in Table 2: the gas metallicity gradient per disc scale length of most models (with the exception of the dynamical time model) is within 10 per cent of the observational average, indicating that gas metallicity gradients have relatively little power to discriminate between the models.

6.4 Comparison with Boissier & Prantzos

Recently, Boissier & Prantzos discussed the properties of a specific, comprehensive disc galaxy spectro-photometric chemical evolution model in a trio of papers (Boissier & Prantzos 1999, 2000; Prantzos & Boissier 2000). They constructed a specific spectro-photometric chemical evolution model that reproduced many observational constraints, and explored why these observational constraints were reproduced by their model. We have taken a complementary approach, where we have explored a wide range of physical processes to understand the effects of each process on the ages and metallicities of spiral galaxies. In this section, we compare the results of our modelling and theirs with a two-fold aim: to check that our studies give consistent results, and to gain some insight into how robust the conclusions of Boissier & Prantzos are likely to be if any of the modelling details were changed.

Their model used a combined Schmidt and dynamical time SFL: $\psi = k\Sigma_{\text{gas}}^{1.5}/\tau_{\text{dyn}}$, including surface density and mass-dependent infall, but, like our models, they did not include gas flows. They used a more sophisticated approach in dealing with the chemical evolution than adopted in this work (they did not use the IRA, but treated the full chemical evolution of the galaxy explicitly). They used halo circular velocities and spin parameters to parameterise their models but did not use the information about halo formation to fully specify the ages and infall histories of the discs they constructed (c.f. Dalcanton et al. 1997; Mo, Mao & White 1998). Instead, they assumed a constant galaxy formation epoch of 13.5 Gyr and tuned the surface density and mass dependence in the infall history to provide as good a match to the observations as possible.

Here, we focus on two issues: the origin of age and metallicity gradients in spirals, and the nature and origin of the mass-metallicity correlation.

One of the main conclusions of Prantzos & Boissier

(2000) is that they required radial variation in both the infall timescale and the SFL to produce colour and metallicity gradients that were large enough to agree with the observations. However, we found earlier that explicit radial dependence of *both* the SFL and infall history is not required to reproduce stellar and gas metallicity gradients, and that radial dependence in either one can produce a sufficient effect.

Another of the significant successes of the model from Boissier & Prantzos (2000) is the reproduction of the metallicity-magnitude correlation. However, at first sight, this is somewhat of a puzzle as they do not include mass-dependent outflows or formation epoch differences in their model: their metallicity-magnitude correlation is reproduced entirely by a mass-dependent infall timescale. This puzzle is resolved by inspection of Fig. 3 of Boissier & Prantzos (2000): it shows that at surface densities typical of spiral discs, the infall prescription that they adopt *increases* with time for galaxies with halo circular velocities $\lesssim 150 \text{ km s}^{-1}$. This increasing infall rate mimics a variation in formation epoch. Therefore, we must modify our earlier conclusions: the infall history at early and intermediate times modifies primarily the colour-based ages of spirals; however, large amounts of late infall affects both the colour-based ages and metallicities of spirals. Furthermore, if the amount of late gas infall depends on galaxy mass, then a metallicity-magnitude relation can be generated. In their model, the metallicity-magnitude relation is generated by differences in galaxy formation epoch (essentially) and so the prediction of a mass-independent effective yield will hold for their model, just as it holds for our mass-dependent formation epoch model.

7 CONCLUSIONS AND PROSPECTS

We have constructed a simple family of chemical evolution models with the aim of gaining some insight into the origins of many of the trends in SFH with galaxy parameters presented in BdJ. The model is used to generate colour-based ages and metallicities, which are directly comparable with those derived in BdJ. We generated a grid of model galaxies and selected only those which lie in a pre-defined region of the K band absolute magnitude–central surface brightness plane.

Using this model, we have found the following:

- A local gas surface density-dependent Schmidt SFL describes many of the colour-based age and metallicity trends from BdJ surprisingly well. A model of this type does not explain the mass dependence in SFH required by BdJ and significantly underpredicts the age gradient in spiral galaxies and the slope of the age–central surface brightness correlation.
- The global properties of the fiducial model can be improved in either of two ways.
 - (i) A combination of mass-dependent infall and metal enriched outflow imprint independent mass correlations on the galaxy colour-based ages and metallicities. Smaller galaxies have a more extended period of inflow in this model, and lose a greater fraction of their freshly-synthesized metals.
 - (ii) Galaxy formation epoch varies systematically with

galaxy mass. If less massive galaxies are younger (i.e. if they assembled the bulk of their gas content at very late times) we explain the mass–metallicity and mass–age correlation without resorting to outflow.

- Regarding the radial variations within galaxies:

- (i) If the infall timescale varies with radius, an age gradient can be generated. This has little or no effect on the metallicity gradient.
- (ii) Alternatively, Kennicutt's (1998) SFL (which involves both gas density and the dynamical time) produces both strong age and gas metallicity gradients and a reasonable scatter in the local age/metallicity–surface brightness correlation. The main shortcoming of this model is a 'backwards' age/metallicity–magnitude correlation.

One deliberate limitation of our empirical approach is that we do not incorporate our model galaxies into a detailed cosmological context. For example, cold dark matter cosmologies make well-defined predictions about the formation mechanisms and infall histories of galactic discs that we ignore (e.g. Steinmetz & Müller 1994; Mo, Mao & White 1998; Somerville & Primack 1999; Cole et al. 2000). A more realistic treatment of the formation of our initial discs would be desirable, but is sensitive to the poorly understood details of angular momentum evolution in forming disc galaxies (e.g. Navarro & Steinmetz 1997; 2000). In this paper our philosophy has been to determine which of our conclusions seem the most robust to model details, and which may change if our initial disc formation was made more realistic. Our study gives an indication of which of our conclusions (and those of Boissier & Prantzos) are robust: i.e. which physical processes must operate in any galaxy formation scenario to reproduce the observations. From the above discussion, we find the following.

- Gas surface density determines the SFR, although other factors (such as dynamical time or a critical density for star formation) may also influence the SFR.
- Radial dependence in the SFL and/or the infall history is favoured.
- The infall of gas *either* varies strongly with galaxy mass, peaking at late times in low-mass galaxies (as parameterised by our formation epoch model, E, or the model of Boissier & Prantzos), *or* infall varies more weakly with galaxy mass but operates in conjunction with a higher efficiency of metal-enriched outflows in low-mass systems (Models I and O). The data (as it stands) marginally favours the latter option (Fig. 6).

However, the last conclusion is strongly dependent on the treatment of very low metallicity galaxies for which our colour-based ages and metallicities are highly uncertain. A combination of models I and O receives further support from studies of resolved stellar populations: there is ample evidence for older stellar populations in local faint, gas-poor and metal-poor dwarf Spheroidal galaxies. These cannot fit into the mass-dependent age scheme postulated above (e.g. Grebel 1998; Hurley-Keller, Mateo & Nemec 1998). Of course, it is quite possible that very low-mass dwarf galaxies have a metallicity–magnitude correlation driven primarily by outflows, and more massive galaxies (such as spirals,

which have managed to keep the bulk of their gas content) have a metallicity–mass correlation driven primarily by differences in galaxy formation epoch. The key observable is the effective yield of galaxies: the effective yield gives insight into whether a galaxy is simply under-evolved and metal-poor (like, perhaps, low surface brightness disc galaxies; de Blok et al. 1996; Bell et al. 2000) or has had the bulk of its metals removed in gas outflows (as appears likely for dwarf Spheroidals: e.g. Dekel & Silk 1986). What is clear is that more work, both on observational and theoretical fronts, is required to fully elucidate the origin of the mass–metallicity correlation.

ACKNOWLEDGEMENTS

We thank the anonymous referee for their helpful suggestions and comments, and Helio Rocha-Pinto for communicating results in advance of their publication. We would like to thank Don Garnett for providing data in electronic form and for his comments on the manuscript. We acknowledge useful discussions with and input from Matthias Steinmetz, Roelof de Jong, Rob Kennicutt and Andrew Benson. EFB acknowledges financial support from the Isle of Man Education Department, NASA grant NAG58426 and NSF grant AST9900789.

REFERENCES

Arimoto N., Yoshii Y., 1987, A&A, 173, 23
 Bell E. F., de Jong R. S., 2000, MNRAS, 312, 497 (BdJ)
 Bell E. F., Barnaby D., Bower R. G., de Jong R. S., Harper D. A., Hereld M., Loewenstein R. F., Rauscher B. J., 2000, MNRAS, 312, 470
 Boissier S., Prantzos N., 1999, MNRAS, 307, 857
 Boissier S., Prantzos N., 2000, 312, 398
 Cole S., Lacey C. G., Baugh C. M., Frenk C. S., 2000, submitted to MNRAS
 Contardo G., Steinmetz M., Fritze-von Alvensleben U., 1998, ApJ, 507, 497
 Dalcanton J. J., Spergel D. N., Summers F. J., 1997, ApJ, 482, 659
 de Blok W. J. G., McGaugh S. S., van der Hulst J. M., 1996, MNRAS, 283, 18
 de Jong R. S., van der Kruit P. C., A&AS, 106, 451
 Dekel A., Silk J., 1986, ApJ, 303, 39
 Disney M. J., Davies J. I., Phillips S., 1989, MNRAS, 239, 939
 Dopita M. A., 1985, ApJ, 295, 5L
 Dopita M. A., Ryder S. D., 1994, ApJ, 430, 163
 Edmunds M. G., 1990, MNRAS, 246, 678
 Edmunds M. G., Greenhow R. M., 1995, MNRAS, 272, 241
 Edvardsson B., Andersen J., Gustafsson B., Lambert D. L., Nissen P. E., Tomkin J., 1993, A&A, 275, 101
 Eggen O. J., Lynden-Bell D., Sandage A. R., 1962, ApJ, 136, 748
 Garnett D. R., Shields G. A., Skillman E. D., Sagan S. P., Dufour R. J., 1997, ApJ, 489, 63
 Grebel E. K., 1998, in "The Stellar Content of the Local Group", Proceedings of IAU Symposium 192, eds. P. Whitelock & R. Cannon
 Huizinga J. E., 1994, PhD Thesis, University of Groningen
 Hurley-Keller D., Mateo M., Nemec J., 1998, AJ, 115, 1840
 Jimenez R., Padoan P., Matteucci F., Heavens A. F., 1998, MNRAS, 299, 123
 Kauffmann G., Charlot S., 1998, MNRAS, 294, 705
 Kennicutt Jr., R. C., 1989, ApJ, 344, 685

Kennicutt Jr., R. C., 1998, *ApJ*, 498, 181 (Ke98)
 Kuchinski L. E., Terndrup D. M., Gordon K. D., Witt A. N.,
 1998, *AJ*, 115, 1438
 Lacey C. G., Fall S. M., 1983, *MNRAS*, 204, 791
 Lacey C. G., Fall S. M., 1985, *ApJ*, 290, 154
 Larson R. B., 1972, *Nature Phys. Sci.*, 236, 7
 Larson R. B., 1976, *MNRAS*, 176, 31
 MacLow M.-M., Ferrera A., 1999, *ApJ*, 513, 142
 Martin C. L., 1999, *ApJ*, 513, 156
 Mo H. J., Mao S., White S. D. M., 1998, *MNRAS*, 295, 319
 Navarro J. F., Steinmetz M., 1997, *ApJ*, 478, 13
 Navarro J. F., Steinmetz M., 2000, *ApJ*, 528, 607
 Pagel B. E. J., 1998, "Nucleosynthesis and Chemical Evolution
 of Galaxies" (Cambridge University Press, Cambridge)
 Peletier R. F., Willner S. P., 1992, *AJ*, 103, 1761
 Persic M., Salucci P., 1991, *ApJ*, 368, 60
 Phillipps S., Edmunds M. G., 1991, 251, 84
 Portinari L., Chiosi C., 1999, *A&A*, 350, 827
 Prantzos N., Aubert O., 1995, *A&A*, 302, 69
 Prantzos N., Boissier S., 2000, *MNRAS*, 313, 338
 Prantzos N., Silk J., 1998, *ApJ*, 507, 229
 Rocha-Pinto H. J., Maciel W. J., 1996, *MNRAS*, 279, 447
 Rocha-Pinto H. J., Maciel W. J., Scalo J., Flynn C., 2000a, sub-
 mitted to *A&A*, astro-ph/0001382
 Rocha-Pinto H. J., Scalo J., Maciel W. J., Flynn C., 2000b, sub-
 mitted to *A&A*, astro-ph/0001383
 Salpeter E. E., 1955, *ApJ*, 121, 61
 Schmidt M., 1959, *ApJ*, 129, 243
 Skillman E. D., Kennicutt Jr., R. C., Hodge P. W., 1989, *ApJ*,
 347, 875
 Somerville R. S., Primack J. R., 1999, *MNRAS*, 310, 1087
 Smartt S. J., Rolleston W. R. J., 1997, *ApJ*, 481, 47L
 Steinmetz M., Müller E., 1994, *A&A*, 281, 97L
 Steinmetz M., Müller E., 1995, *MNRAS*, 276, 549
 Tinsley B. M., 1980, *Fundamentals of Cosmic Physics*, Vol.5,
 p.287
 Tinsley B. M., Larson R. B., 1978, *ApJ*, 221, 554
 Toomre A., 1964, *ApJ*, 139, 1217
 Tully R. B., Verheijen M. A. W., Pierce M. J., Huang J., Wain-
 scoff R. J., 1996, *AJ*, 112, 2471
 Tully R. B., Pierce M. J., Huang J., Saunders W., Verheijen M.
 A. W., Witchalls P. L., 1998, *AJ*, 115, 2264
 Twarog B. A., 1980, *ApJ*, 242, 242
 Vilchez J. M., Esteban C., 1996, *MNRAS*, 280, 720
 Worthey G., Dorman B., Jones L. A., 1996, *AJ*, 112, 948
 Wyse R. F. G., Silk J., 1989, *ApJ*, 339, 700